PROTON BEAM APPLICATIONS FOR SILICON BULK MICROMACHINING

P. Nenzi, G. Bazzano, F. Marracino, L. Picardi, C. Ronsivalle, V. Surrenti, M. Vadrucci, ENEA
C.R. Frascati, Frascati, Italy
C. Snels, M. Tucci, ENEA Casaccia, Roma, Italy
F. Ambrosini, M. Balucani, A. Klysko, DIET - University «La Sapienza», Roma

Abstract

We have investigated the effects of deep hydrogen implantation into *n*- and *p*-type silicon wafers ((100) oriented, with resistivity in the 1-20 $\Omega\cdot$cm range). Deep implantation has been achieved using the Hitachi-AccSys PL-7 RF LINAC set for 3.0 MeV beam energy, degraded to 1.8 MeV. Hydrogen has been implanted 30 µm below the wafer surface with an implant dose (fluence) >5x10^{15} cm^{-2}. Samples were partly covered by a metal mask during implant. Porous silicon has been formed on the exposed samples to study the effect of hydrogen irradiation. We have found that porous silicon formation is inhibited in the irradiated areas on *p*-type silicon and promoted on the *n*-type one.

INTRODUCTION*

Ion implantation into semiconductors is one of the key industrial applications of particle accelerators. Figure 1 shows the most common implantation energies, doses, and chemical species, employed in the semiconductor industry.
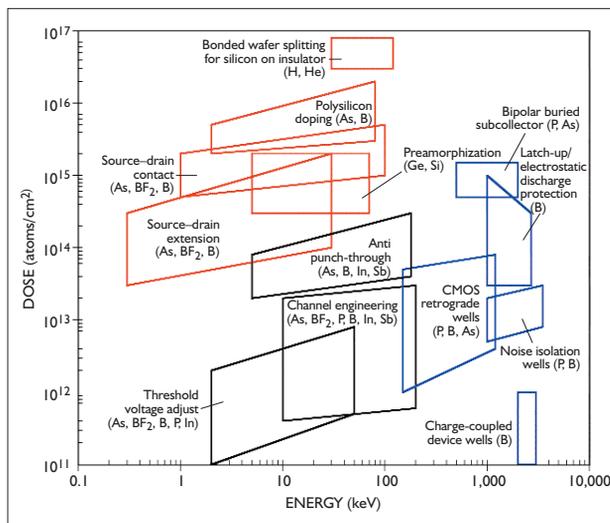

Figure 1: Process and dose application space for semiconductor industry. Hydrogen implantation has been used mainly for the manufacturing of SOI wafers where doses in excess of 5x10^{16} are required.

Hydrogen implantation has been historically relegated to the manufacturing of SOI (Silicon-On-Insulator) wafers [1, 2] and, more recently, in the bulk micromachining of silicon in conjunction with the formation of porous silicon [3, 4].

CEA LETI has commercially exploited hydrogen implantation since 1994 [2] for the production of SOI wafers. The technique, known with the name "smart cut", uses protons (H^{+} ions) to create lattice defects in correspondence of the stopping range. In this technology, 150 keV protons are used, corresponding to an implantation peak at 1.25 µm below the surface. A layer with dopant concentration of 10^{16} cm^{-3} has been achieved with implant dose (fluence) higher than 5x10^{16} cm^{-2}.

When the above concentration is reached it is possible to thermally trigger the coalescence of the defects to create "bubbles" in the silicon crystal and cleave the wafer along a plane parallel to its surface in a position corresponding to the stopping range.

Silicon micromachining technologies, based on hydrogen irradiation, follows the discovery that, irradiated areas cannot be converted into porous silicon [3]. The starting material was *n*- and *p*-type silicon 0.015-0.020 $\Omega\cdot$cm and 0.010-0.020 $\Omega\cdot$cm, respectively, and the proton energy was 2 MeV. The authors attributed that behavior to the defects induced by the proton beam in the silicon crystal. A more recent explanation of this phenomenon has been given in [5], in which the authors attribute the suppression of porous silicon formation to defect induced by the beam to *holes* transport through the lattice (porous silicon formation requires continuous *holes* supply). They simulated hole current of an irradiated structure into silicon using a commercial finite elements code (COMSOL) solving the Poisson's and continuity equation (in two dimensions) at different biases and verified their results experimentally.

In such technologies, porous silicon is used as sacrificial material, due to its etching selectivity with respect to silicon (up to 1x10^{5}:1, for potassium hydroxide (KOH) etch). In such technologies [4], silicon is patterned with a focused proton beam, e.g. Nuclear Microprobe [6], (essentially an high energy Focused Ion Beam) with a spot size of 200 nm to locally induce defects into the silicon lattice. Protons (or He ions) with energies in the range 0.25 MeV to 2 MeV at fluencies between 5x10^{14} cm^{-2} to 5x10^{15} cm^{-2} are employed. Complex three-dimensional structures can be realized with such technologies [7].

In our experiment we focused on lowly doped silicon wafers (p^- type 1-10 Ω·cm and n^- type 20 Ω·cm). The p-type wafer doping level was chosen because of its low cost and the possibility to grow macroporous silicon, a morphology that can be exploited for the realization of silicon interposers for integrated circuit packaging [8].

The lowly-doped n-type wafer was chosen because porous silicon does not grows on that type of wafer and, by proton irradiation we would promote its growth in irradiated areas (a behavior complementary to the one exhibited by p-type wafers).

EXPERIMENTAL SETUP

The TOP-IMPLART facility [9-14] has been used to carry out the experiments. TOP-IMPLART is a proton pulsed linear accelerator under construction at the ENEA Frascati Research Center, whose primary application will be intensity-modulated protontherapy. The accelerator, at the actual stage of development, is composed by a commercial (Hitachi-AccSys PL7) injector that can reach a energy of 7 MeV and an S-Band SCDTL-type LINAC that reaches 11.6 MeV connected through a Low Energy Beam Transfer (LEBT) line including four quadrupoles. The versatility of a modular scheme allows it to be set to perform different experiments on biological and inorganic samples [15, 16].

In silicon irradiation experiments, the LINAC is operated at 3 MeV (by powering only the RFQ section of the injector). The sample is placed the end of the injector, in the middle of the LEBT before the SCDTL section, after the first quadrupole doublet in a specially designed holder (see Figure 2) that seals the accelerator's pipe and gives access to thermocouple contacts and electrical contacts for beam current measurement.
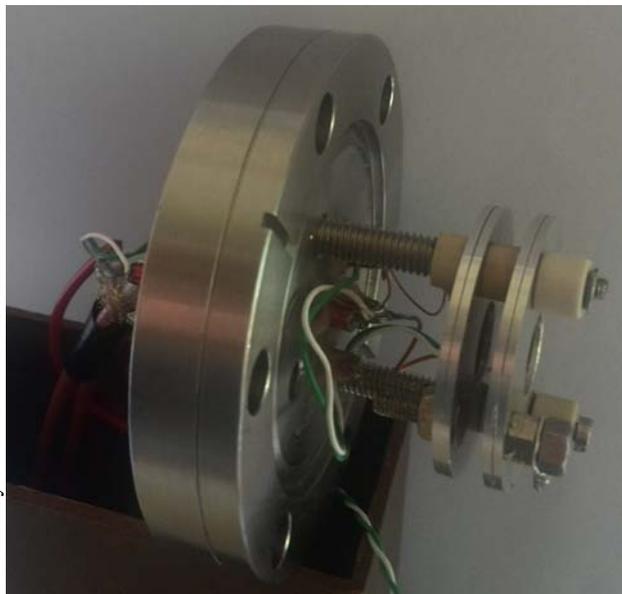

Figure 2: Sample holder built onto a blind flange. Silicon sample is placed below an aluminum degrader that reduces the beam energy from 3.0MeV to 1.8 MeV. Current and temperature are monitored.

Figure 3 depicts the experimental setup. In our experiments we appropriately de-focused the beam using the quadrupoles to obtain a uniform beam over a 1.0 cm^2 area at the position of the silicon sample. The 3 MeV beam is degraded by 60 µm thick aluminum foil to 1.8 MeV, the experiment energy. The silicon sample is masked with a 200 µm thick metal (molybdenum) mask that defines a regular pattern (parallel lines 500 µm wide separated by 500 µm gap) over the silicon wafer.
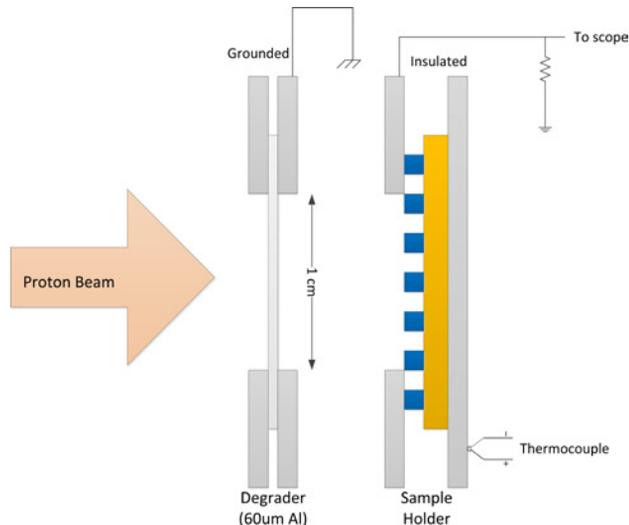

Figure 3: Silicon irradiation setup. The sample is positioned after the aluminum degrader and masked with a Molybdenum mask to define a regular pattern on its surface. Silicon temperature and beam current is measured.

The temperature reached by the silicon sample is continuously monitored by a K-type thermocouple installed in the back of the holder in close contact with the silicon wafer. The current is also monitored and integrated to compute the fluence. The TOP-IMPLART control system has been upgraded to stop the irradiation process once the prescribed charge has been accumulated.

The TOP-IMPLART machine was operated at a pulse length of 98 µs and a pulse repetition frequency of 30 Hz, with an estimated charge/pulse of 8.91×10^{-9} C (corresponding to 5.57×10^{10} protons/pulse). Our target fluence ($> 5 \times 10^{15}$ cm^{-2}) requires 3600 s of irradiation. Four silicon samples of each doping type were irradiated for 4500 s to reach the expected fluence (this difference is due to instability of the current of the injector).

EXPERIMENTAL RESULTS

The first experiments were carried on p-type samples. The four samples have been irradiated with a fluence of 6×10^{15} cm^{-2} obtaining a concentration peak at the stopping range of 7.2×10^{19} cm^{-3} (as computed by SRIM/TRIM Monte Carlo code [17]). The temperature reached by the samples did not exceed 120 °C. Hydrogen implant has been confirmed by FTIR analysis (see Figure 4), acquired with a Perkin-Elmer Frontier FTIR

spectrometer. The baseline correction has been done by acquiring the spectrum of silicon in a non-irradiated portion of the sample (i.e. at the border).

The spectrum has not been normalized and the amplitude is in "arbitrary-units". Peaking behavior near hydrogen lines is visible.
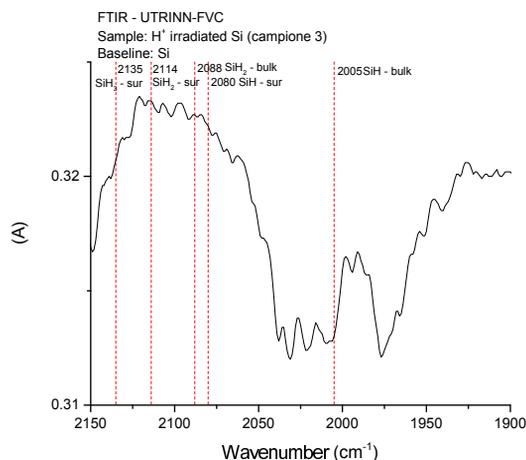

Figure 4: FTIR analysis of p-type sample. The spectrum has not been normalized and the amplitude is in "arbitrary-units".

Porous silicon has been grown using a mixture HF:IPA=1:1 (48 wt% hydrofluoric acid (HF) mixed in equal part with isopropyl alcohol (IPA)) in galvanostatic regime at 20 mA/cm^2 current density.

Mesoporous silicon has been grown in masked areas and removed by KOH etch to delineate the implantation profile. Figure 5 (obtained with Zeiss Auriga FESEM) shows that irradiation prevented porous silicon growth up to 32 µm (the cross-sectional image has been taken at angle (27°) and 1.22 correction factor must be applied to measurements).
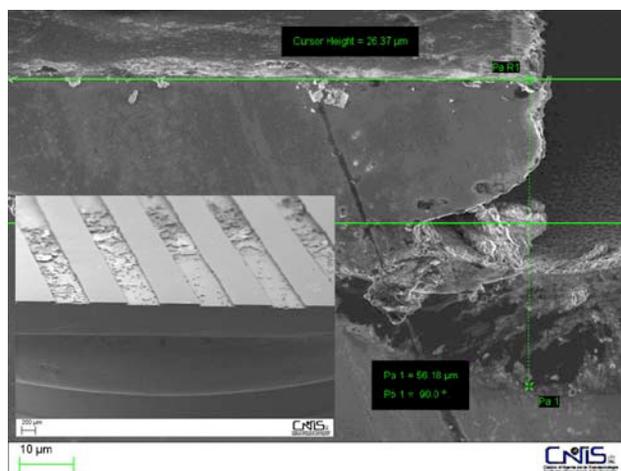

Figure 5: Pattern transferred to p-type silicon sample. The image shows the border of an etched area (porous silicon removed by KOH etch). Inset shows a lower magnification image of the same sample, displaying the transferred pattern.

Porous silicon growth has been obtained on n-type samples by using a HF:DI:IPA=1:3:1 mixture (48 wt% HF diluted in deionized water (DI) and IPA). Current density was set at 30 mA/cm^2 (in dark condition). Porous silicon grows in the irradiated areas (see Figure 6). The growth process has not yet been optimized for this type of wafer and some of the samples were electropolished.
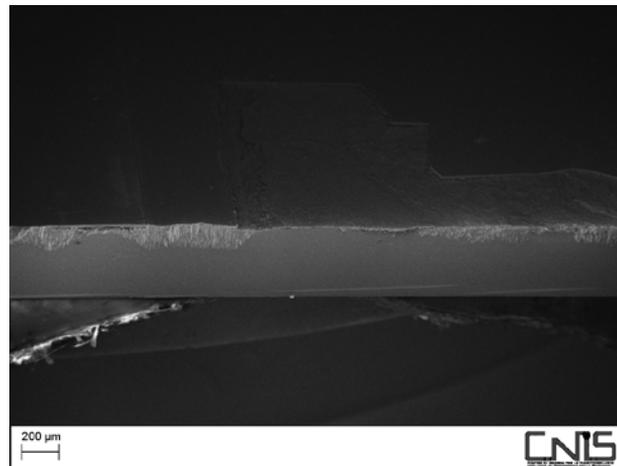

Figure 6: Pattern transferred on the *n*-type sample. Porous silicon has not been etched and is visible as a bright area in the cross-section with the typical columnar morphology.

CONCLUSION

In this work we have demonstrated a novel technology for silicon micromachining that is particularly interesting for large area applications, as in integrated circuit package design. The use of a metal mask to transfer a pattern, instead of a scanned focused beam, allows higher throughput in industrial applications. Moreover, the possibility of deep implantation (using MeV beams), up to 75, opens new ways to the realization of through-wafer structures (as trough-silicon vias).

We have obtained a complementary behavior on *n*-type and *p*-type wafers: porous silicon grows in irradiated areas on *n*-type and in masked areas on *p*-type. The growth process has been optimized for the *p*-type and requires further studies on the *n*-type as it is too prone to electropolishing.

REFERENCES

[1] B. Aspar, M. Bruel, H. Moriceau, C. Maleville, T. Poumeyrol, A.M. Papon, et al., "Basic mechanisms involved in the Smart-Cut$^{(R)}$ process", Microelectronic Engineering, 36(1-4), pp. 233–240, 1997.

[2] B. Michel, "Process for the production of thin semiconductor material film", Patent No. US5374564, Dec. 1994.

[3] A. Polesello, C. Manfredotti, F. Fizzotti, R. Lu, E. Vittone, G. Lerondel, A. M. Rossi, G. Amato, L. Boarino, S. Galassini, M. Jaksic, Z. Pastuovic,

"Micromachining of silicon with a proton microbeam", Nucl. Instr. And Meth. B, 158, pp. 173-178, 1999.

[4] S. Azimi, M.B.H. Breese, Z.Y. Dang, Y. Yan, Y.S. Ow, A.A. Bettiol, "Fabrication of complex curved three-dimensional silicon microstructures using ion irradiation", J. Micromech. Microeng, 22(1), 015015, 2012.

[5] Z.Y. Dang, J. Song, S. Azimi, M.B.H. Breese, J. Forneris, E. Vittone, "On the formation of silicon wires produced by high-energy ion irradiation", Nucl. Instr. And Meth. B, 296, pp. 32-40, 2013.

[6] M. B. H. Breese, G. W. Grime, F. Wat, "The Nuclear Microprobe", Annu. Rev. Nucl. Part. Sci., 42:1-38, 1992.

[7] S. Azimi, J. Song, Z .Y. Dang, H.D. Liang, M.B.H. Breese, "Three-dimensional silicon micromachining" , J. Micromech. Microeng., 22, 113001, 2012.

[8] P. Nenzi, K. Kholostov, R. Crescenzi, H. Bondarenka, V. Bondarenko, M. Balucani, "Electrochemically etched TSV for porous silicon interposer technologies," Electronic Components and Technology Conference (ECTC), 2013 IEEE 63rd, pp. 2201-2207, 28-31 May 2013.

[9] C. Ronsivalle et al. "The TOP IMPLART Project", Eur. Phys. J Plus (2011) 126, no. 7,68.

[10] C. Ronsivalle et al., "Simple characterization method of small high gradient permanent magnet quadrupoles", Proceedings of IPAC2014, Dresden, Germany, pp. 1250-1252.

[11] L. Picardi et al. "Experimental results on SCDTL structures for protons", Proceedings of IPAC2014, Dresden, Germany, pp. 3247-3249.

[12] C. Ronsivalle et al. "First acceleration of a proton beam in a Side Coupled Drift tube Linac", submitted to Europhysics Letters.

[13] P. Nenzi et al., "Status of the TOP-IMPLART Proton LINAC", TUPWI004, these proceedings, IPAC '015, Richmond (VA), USA (2015).

[14] V. Surrenti et al., "RF System Design for the TOP_IMPLART Accelerator", MOPHA047, these proceedings, IPAC '015, Richmond (VA), USA (2015).

[15] M. Vadrucci et al., "Experimental activity in the ENEA-Frascati irradiation facility with 3-7 MeV protons", Proceedings of IPAC2014, Dresden, Germany, pp. 2156-2158.

[16] M. Vadrucci et al., "Proton Irradiations of Micro-TOM Red Hairy Roots to Mimic Space Conditions", TUPWI005, these proceedings, IPAC '015, Richmond (VA), USA (2015).

[17] J.F. Ziegler, J.P. Biersack, M.D. Ziegler, "SRIM - The Stopping and Range of Ions in Matter", Nucl. Inst. Metth. Phys B, 268 (11-12), pp. 1818-1823, 2010.